JOTCS
Journal of the Turkish Chemical Society
Section: A
Chemistry
TURKISH CHEMICAL SOCIETY

Biosorption Studies of Mushrooms for Two Typical Dyes

Ayfer YILDIRIM[1*], Hilal ACAY [2]

[1]Vocational Higher School of Health Services, Mardin Artuklu University, Mardin, Turkey
[2]Department of Nutrition and Dietetics, Faculty of Health, Mardin Artuklu University, Mardin, Turkey

Abstract: This study investigated the adsorption behaviour of two cationic dyes, methylene blue (MB) and malachite green (MG) onto *Pleurotus ostreatus*, *Armillaria tabescens,* and *Morchella conica* mushrooms. The effects of contact time, initial dye concentration, and solution pH (3-11) were also determined. The adsorption on all mushrooms attained equilibrium within 120 min for both MB and MG. To evaluate the experimental kinetics data, the pseudo-first-order, pseudo-second-order, and intraparticle diffusion kinetics equations were utilised. The pseudo-first-order kinetic model demonstrated a good fit with all adsorption kinetics. The Langmuir and Freundlich isotherm models were used to analyse the mechanism of the adsorption isotherm. The adsorption equilibrium isotherm was in a good agreement with the Freundlich model. Thermodynamic parameters such as ΔH enthalpy variation, ΔS entropy variation, and ΔG free Gibbs energy variation were calculated at 303-323 K. The results suggested that the *Pleurotus ostreatus* mushroom was the most suitable adsorbent for both cationic dyes' removal.

Keywords: Mushroom, biosorption, methylene blue, malachite green, thermodynamic parameters.

Submitted: June 21, 2019. **Accepted:** January 19, 2020.

Cite this: Yıldırım A, Acay H. Biosorption Studies of Mushrooms for Two Typical Dyes. JOTCSA. 2020; 7(1): 295-306.

DOI: https://doi.org/10.18596/jotcsa.581007.

***Corresponding author. E-mail**: ayferyildirim@artuklu.edu.tr. **Tel**: +90 482 213 4002/7261

INTRODUCTION

Dyes that are used in the food, textiles, paper, plastics, cosmetics, pharmaceuticals, and other industries generally have carcinogenic, mutagenic, and teratogenic properties. This is why they can cause serious environmental problems (1,2).

Among the techniques used to remove dye molecules from wastewater, adsorption has been recognised as the most effective one as it is proven to be practical and low-cost and have high efficiency (3). However, it has been reported that most sufficient adsorbents such as activated carbon are costly in overcoming the pollution problems of dyes. Thus, the high cost of commercial adsorbents has encouraged researchers to investigate non-toxic, low-price, biodegradable, and environment-friendly alternative biosorbent materials (4). In general, these materials include natural biosorbents derived from waste materials from industries and agriculture. White rot fungi are the most commonly used organisms in biological treatment studies in the field of waste and environmental biotechnology (5). Among them, the Basidiomycetes group takes a great part in the organic compound oxidation of very different molecular structures with various enzymes synthesised mainly by the laccase enzyme, which increases because of intensive industrial activity and environmental annihilation and pollution (6). These mushrooms draw great attention with their properties and have been used in many biotechnological studies. The most commonly used white fungi species include *Phanerochaete chrysosporium, Coriolus versicolor,* and *Trametes versicolor* as well as *Funalia trogii*, *Pleurotus ostreatus*, *P. sajor-caju* and *P. eryngii*, (7,8). It has been reported in the studies in the literature that these mushrooms have been widely used all over the world to eliminate the color of textile wastewaters (9-11).

Pleurotus ostreatus (M1) and *Armillaria tabescens* (M2), which are the mushroom species used in the present study, are white-rot fungi and in the

basidiomycetes group while *Morchella conica* (M3), the other species used in this study, is not white-rot fungi and in the ascomycetes group. To the best of our knowledge, no study has been reported on the adsorption behaviours of Methylene blue (MB) and Malachite green (MG), both cationic dyes, by these three edible fungi (M1, M2, and M3). The influence of kinetics, contact time, pH and initial dye concentration on the adsorption capacity was evaluated and discussed. By using the Freundlich and Langmuir isotherms, the equilibrium data were analysed and characteristic parameters were determined.

MATERIALS AND METHODS

Preparation of the biosorbent

The M1, M2 and M3 mushrooms used in this study were obtained from the province of Mardin in Turkey between April-May 2016. The mushrooms were identified according to Phillips (1994) using ecological, macroscopic and microscopic data. The mushrooms were dried at room temperature for four days. The dried mushroom samples were pulverised in a mixer to be used in the experimental studies.

Preparation of the adsorbate

MB was purchased from Merck while MG was purchased from Sigma. The other reagents used were of analytical grade and all solutions were prepared with distilled water.

Characterisation methods

The characterisation of the mushrooms was achieved by differential scanning calorimetry (DSC) measurements that were performed on a TA Instruments DSC250 with a heating rate of 10 °C min^{-1} under nitrogen atmosphere and Fourier-transform infrared (FTIR) spectra which were recorded on ALPHA Bruker spectrometer with a Platinum-ATR accessory (ZnSe crystal).

Kinetic and equilibrium biosorption studies

1000 mg L^{-1} of the dyes were prepared in distilled water to obtain stock solutions and, by using the stock solutions, the required concentrations were achieved with dilution. The current pH was adjusted by 0.1 N HCl and 0.1 N NaOH solutions.

To investigate the kinetics of the biosorption ability of the three fungal biosorbents on the MB and MG dyes, batch experiments were carried out typically, using 50 mg biomasses, 50 ml of dye solutions (25-75 mg L^{-1}) in 100 mL glass flask with an agitation speed of 120 rpm (GFL 1083 model thermostatted shaker) at natural pH at 303 K for certain times (30, 60, 90, 120, 150, 180, 240 min). The dyes' concentration in aqueous solution was measured at a max wavelength of 632 (MB) and 617 (MG) nm using PG T80+ Model UV-Visible spectrophotometer.

The concentration retained in the fungal biomasses phase was calculated by the following equation:

$$q=(C_0-C_e)\ V/m$$

Where q is the amount of the dye adsorbed per unit weight of the biosorbent (mg g^{-1}), C_0 is the initial concentration of the dye (mg L^{-1}), C_e is the concentration of the dye in solution at equilibrium time (mg L^{-1}), V is the solution volume (L) and m is the weight of the mushrooms (g).

RESULTS AND DISCUSSION

Characterisation of mushrooms

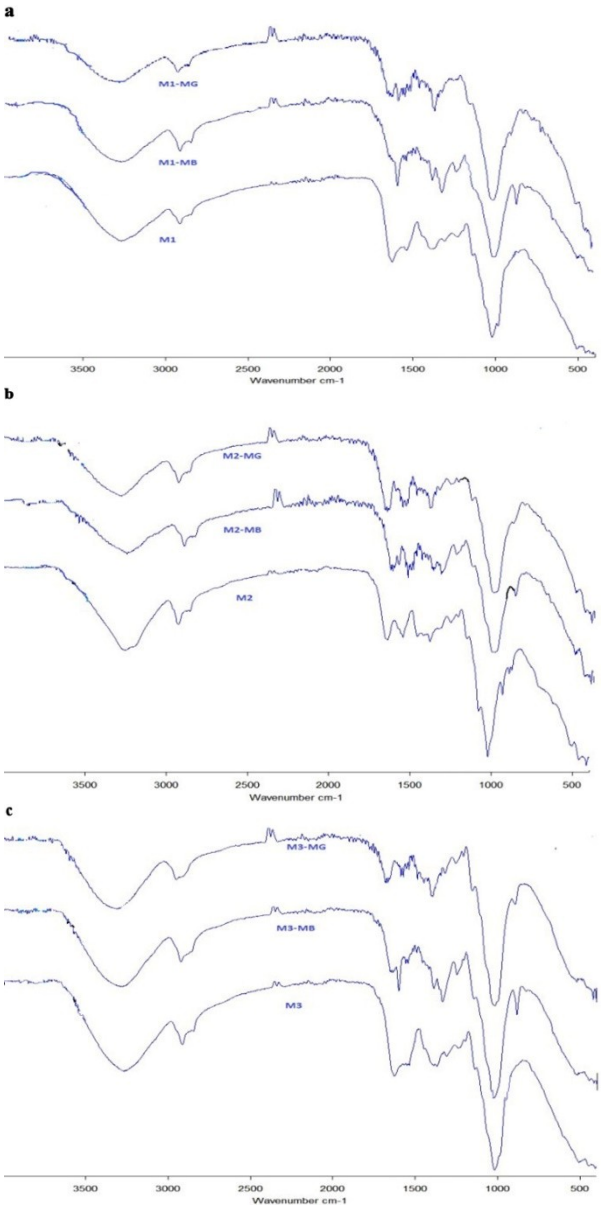

Figure 1. FTIR spectra of M1, M2, M3 and MB, MG loaded **a**:M1 **b**:M2 **c**:M3.

The chemical structures of the mushrooms were confirmed by determining the functional groups in their structures using FTIR spectroscopic analysis (Fig.1a-c.). The FTIR spectra of the mushrooms were found to demonstrate characteristic amine absorption peak around 1600 cm^{-1}. The C–H stretch peak around 2900 cm^{-1} and broad peaks at 3500–3100 cm^{-1} are attributed to N–H and OH–O stretching. Besides, the amide I peak (1700–1600

cm−1) is known to provide information about the C=O stretching of amide groups (Fig. 1a-c.) (12,13). According to Figure 1a-c, the peak at 1633.93 cm^{-1} (M1), 1635.93 cm^{-1} (M2) and 1635.65 cm^{-1} (M3) is typical of a C-N and N-H deformations that shifted to 1597.25 cm^{-1}, 1636.48 cm^{-1} and 1633.36 cm^{-1} after MB adsorption and shifted to 1635.45 cm^{-1}, 1646.60 cm^{-1} and 1647.09 cm^{-1} after MG adsorption.

The presence of peaks at 1393.69 cm^{-1}, 1326.11 cm^{-1} (M1), 1374.93 cm-1, 1339.26 cm^{-1} (M2) and 1374.58 cm^{-1}, 1317.73 cm^{-1} (M3) is attributed to COO^- vibration in carboxylates that shifted to 1386.11 cm^{-1}, 1328.78 cm^{-1}; 1386.99 cm^{-1}, 1338.17 cm^{-1}; 1386.49 cm^{-1}, 1333.90 cm^{-1} and increased after the adsorption of MB and shifted to 1395.97 cm^{-1}, 1339.18 cm^{-1}; 1396.16 cm^{-1}, 1339.38; 1396.43 cm^{-1}, 1339.60 cm^{-1} after MG adsorption which indicated the presence of MB and MG molecules adsorbed (C=C of the alkyl R-). The peaks observed at 1028.70 cm^{-1} (M1), 1021.50 cm^{-1} (M2) and 1026.94 cm^{-1} (M3) cm^{-1} are attributed to the C-O stretching of alcohol and carboxylic acids that shifted to 1017.76 cm^{-1}, 1006.14 cm^{-1} and 1026.94 cm^{-1} after the adsorption of MB and shifted to 1008.46 cm^{-1}, 1020.71 cm^{-1} and 1012.88 cm^{-1} after the adsorption of MG dye molecules (14-18).

The peak at 899.82 cm^{-1} (M2) shifted to 884.09 cm^{-1} after MB adsorption and shifted to 878.72 cm^{-1} after MG adsorption while new peaks at 883.66 cm^{-1} (M1) and 884.52 cm^{-1} (M3) were formed after the adsorption of MB at 885.14 cm^{-1} (M1), 867.01 cm^{-1} (M3) after the adsorption of MG belongs to the C-H out of plane bending vibration of an aromatic ring (Fig. 1a-c.) (19-21).

The change and shift in the intensity of the characteristic peaks in the hybrid spectra after adsorption could also be evidence of interactions between the functional groups of the mushrooms and dye molecules (22).

Figure 2 shows the DSC measurements which determined the thermal behaviour of the mushrooms. The samples were heated from -50 °C to 250 °C at a heating rate of 10 °C/min under an inert atmosphere of nitrogen. There was an endothermic peak of each mushrooms appearing at 92.39 °C (M1), 82.56 and 143.80 °C (M2) and 92.32 °C (M3) while enthalpy was 236.36 J/g (M1), 169.39 and 4.1701 J/g (M2) and 268.51 J/g (M3), respectively. The endothermic process mainly contained hydrogen bond dissociation and water loss. Thus, the endothermic peak of M2 presented the highest value due to slow water loss, increasing thermal stability. This may be caused by the fact that M2 is from a different group of species and has a different chemical composition and physical properties (such as density) (23,24).

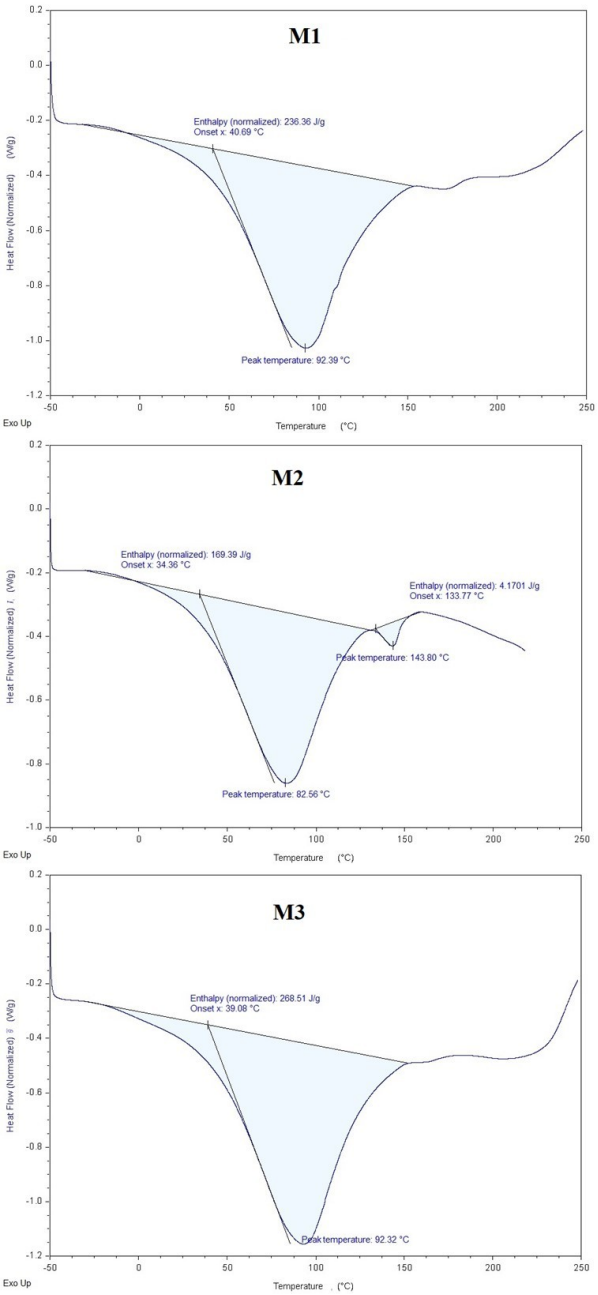

Figure 2. The DSC plots for the mushrooms investigated.

The effect of contact time

The adsorption capacity of two cationic dyes increased with contact time and reached equilibrium about 240 min with a fixed V=50 mL, C_0=25, 50, 75 mg L^{-1}, m=0.01 g and r=120 rpm (Fig.3a,b).

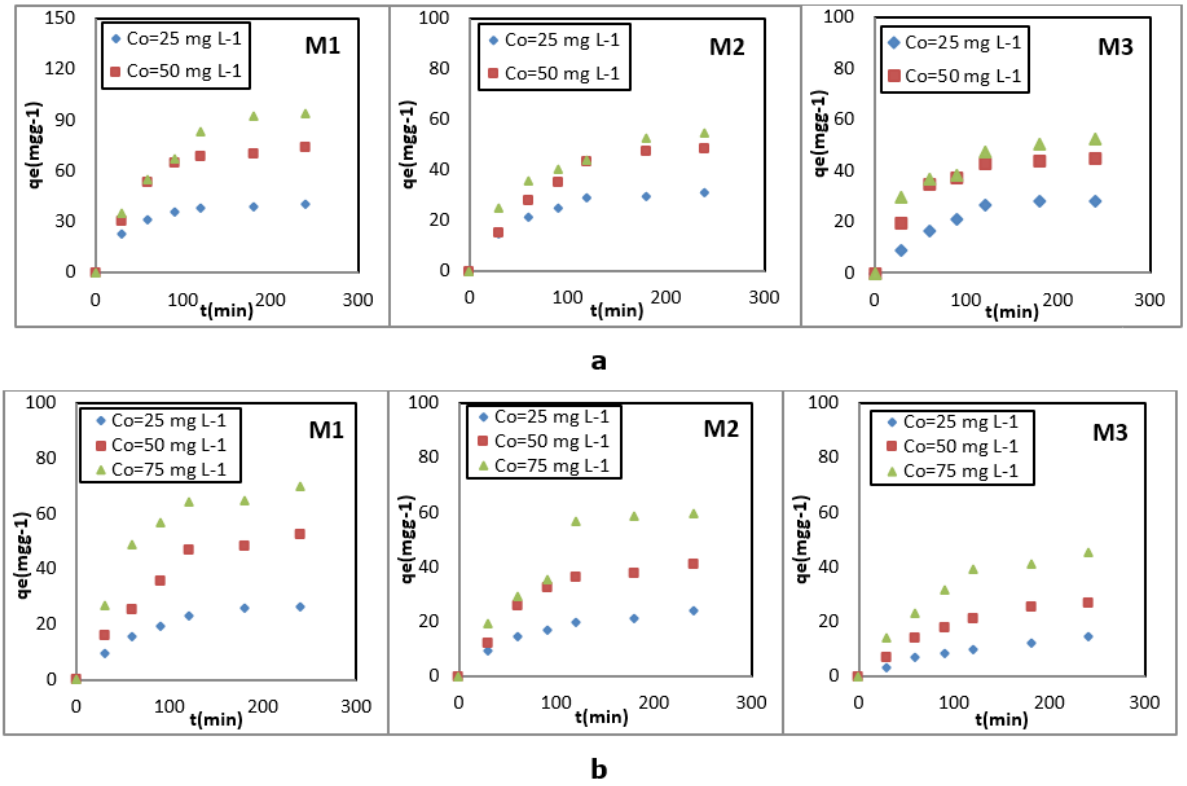

Figure 3. Effect of contact time on the adsorption of **a:** MB, **b:** MG onto M1, M2, M3.

According to Figure 3a-b, the q_e was (for Co=25, 50, 75 mg L^{-1}) 38.48, 68.77 and 82.81 mg g^{-1} for M1; 28.96, 43.20, 43.90 mg g^{-1} for M2 and 26.63, 36.45, 38.47 mg g^{-1} for M3 with the adsorption of MB while it was 23.10, 47.02, 64.13 mg g^{-1} for M1, 19.80, 36.17, 56.80 mg g^{-1} for M2 and 9.98, 20.92, 39.28 mg g^{-1} for M3 with the adsorption of MG respectively. This result suggests that M1 is a more appropriate adsorbent than M2 and M3 (M1>M2>M3) for the effective removal of both MB and MG dyes. Besides, Table 4 shows the comparison of the adsorption capacities of MB and MG cationic dyes onto M1, M2, M3 with the biosorbents in the literature.

Effect of pH

pH can significantly affect the adsorption process. To study the influence of pH on the adsorption capacity of the mushrooms, experiments were performed under the pH range from 3 to 11. It was found that the adsorption amount of MB increased with increasing pH from 3 to 11 while MG adsorption increased rapidly at a low pH value (3-6) and increased further in the range of pH from 6 to 12 (Fig. 4a,b). At a low pH (in acidic media), repulsion activities occurred greatly between cationic dyes (MB, MG) ions and positively charged groups on the surface of the mushrooms. On the contrary, with increasing pH, electrostatic attractions between cationic dye ions and negatively charged sites on mushrooms' surface were enhanced both cationic dyes adsorption (25-28). These results indicate that the adsorption of MG is more influenced by pH change than the adsorption of MB on the surface of mushrooms.

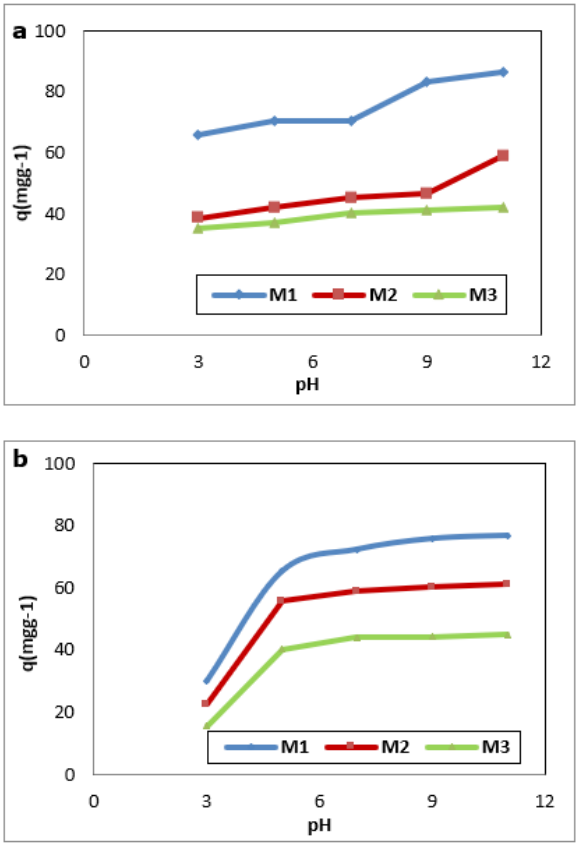

Figure 4. Effect of pH on the adsorption **a:**MB, **b:**MG on the M1, M2, M3.

Evaluation of biosorption kinetics

Two kinetic models, namely pseudo-first-order equation and pseudo-second-order equation were used to investigate the adsorption kinetic

behaviors of MB and MG onto three mushrooms. To estimate the suitability of the models, it is necessary to introduce the correlation coefficient (R~1). The higher R^2 value indicates a more applicable model to the kinetics of dye adsorption.

The pseudo-first-order kinetic model is expressed by the equation 1 (29):

$$\log(q_e - q_t) = \log(q_e) - k_{1t} \quad (1)$$

where q_e and q_t refer to the amount of MB and MG adsorbed (mg g^{-1}) at equilibrium and at any time t(min), respectively, and k_1 is the equilibrium rate constant of pseudo-first-order (min^{-1}).

k_1 is the equilibrium rate constant of pseudo-first-order model which was calculated by the slope and intercept of the plot of $\log(q_e - q_t)$ versus t (Fig. 5a,b).

The pseudo-second-order model which is expressed by equation 2 (30):

$$t/qt = 1/k_2 q^2_e + t/q_e \quad (2)$$

Where, k_2 is the equilibrium rate constant of pseudo-second-order (g mg^{-1} min^{-1}) which can be determined by the slope and intercept of the plot of t/q_t versus t (Fig. 6a,b).

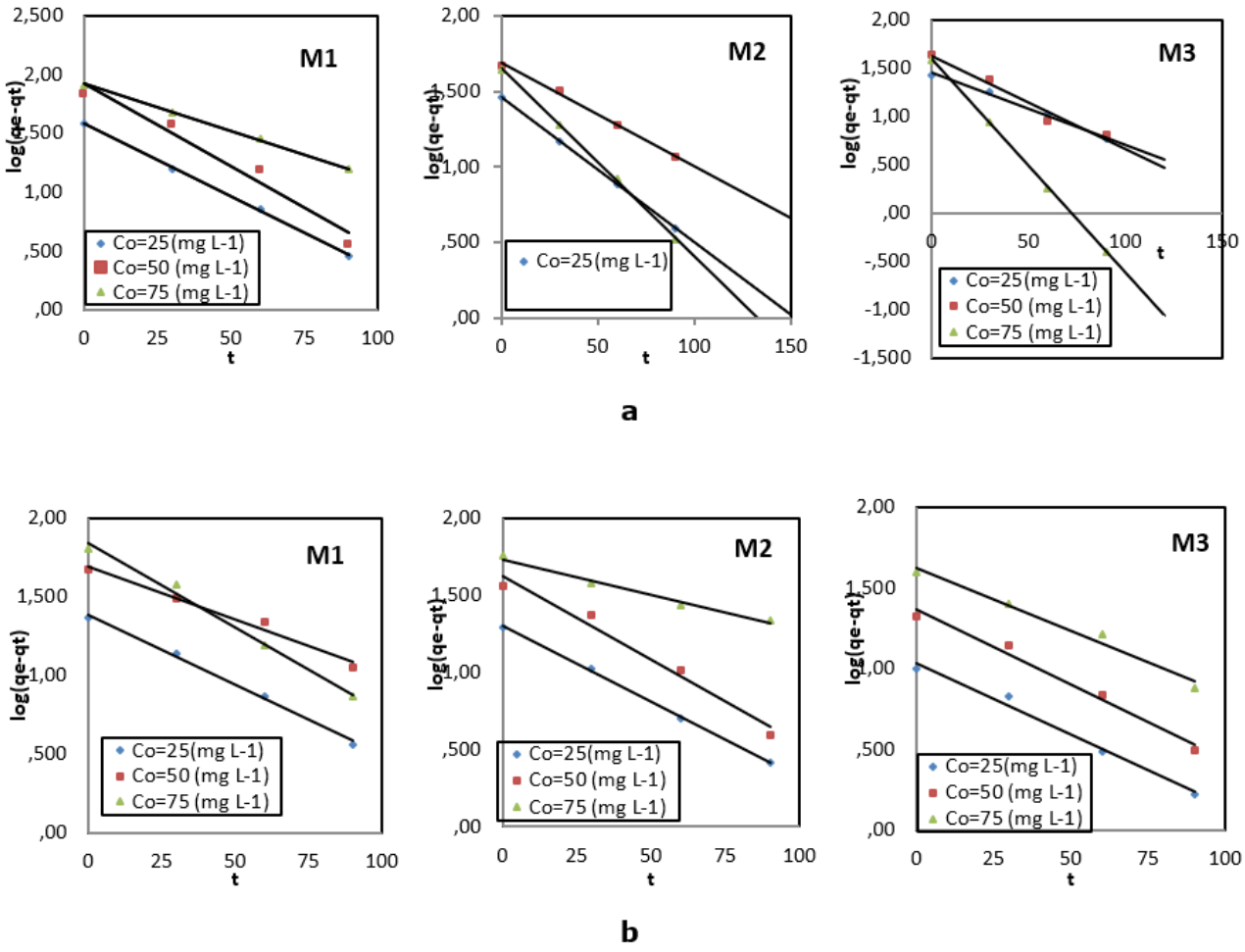

Figure 5. Plots for the pseudo-first-order kinetic model **a:**MB adsorption, **b:**MG adsorption.

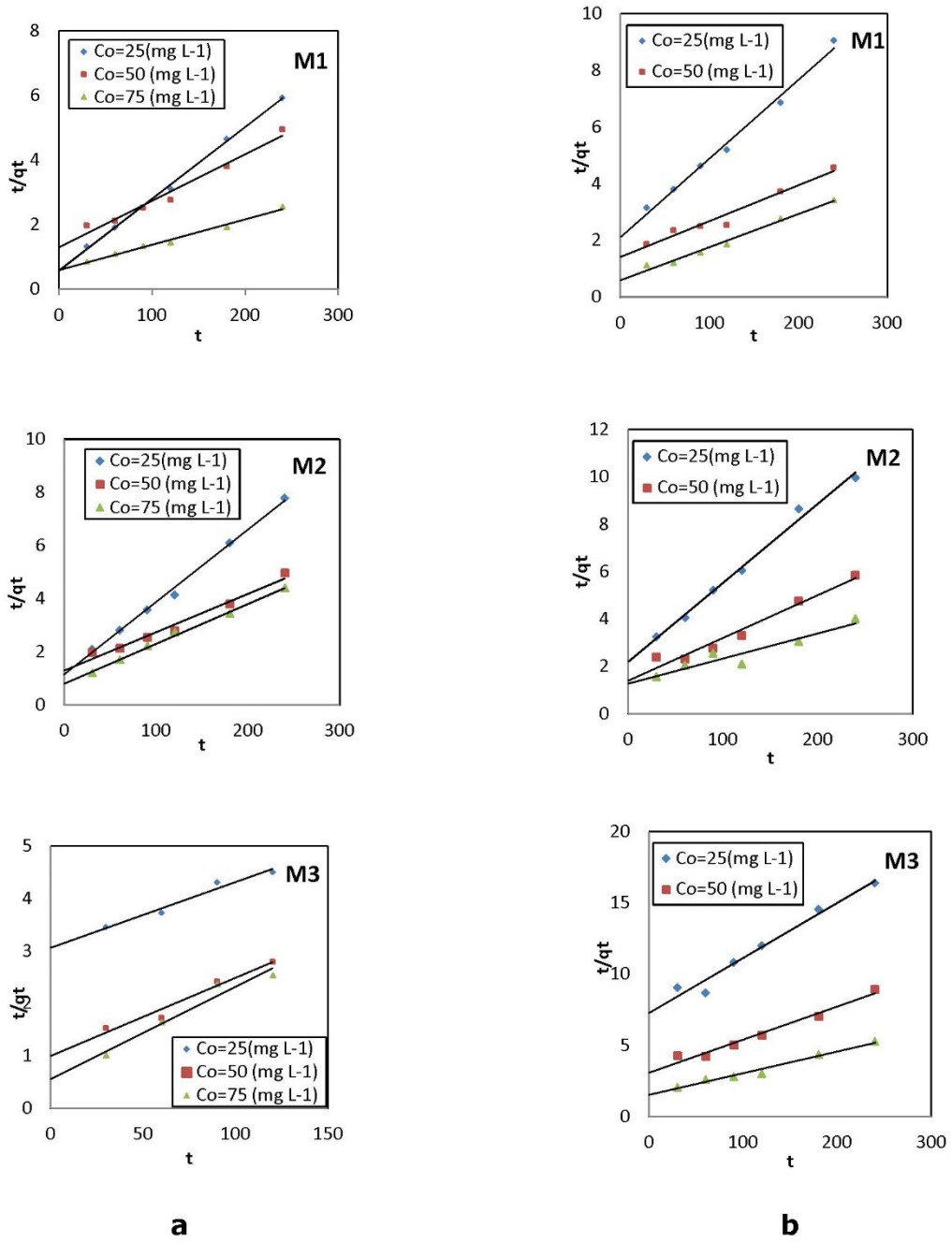

Figure 6. Plots for the pseudo-second-order kinetic model a:MB adsorption b:MG adsorption.

Table 1. Parameters for pseudo-first and second-order kinetic models

Dye	Adsorbent	Co (mg L^{-1})	q_e.exp (mg g^{-1})	Pseudo-first			Pseudo-second		
				q_e.c (mg g^{-1})	k_1 (min^{-1})	R^2	q_e.c (mg g^{-1})	k_2 (g mg^{-1} min^{-1})	R^2
MB	M1	25	38.48	38.26	0.0286	0.999	44.84	1.7379	0.990
		50	68.77	71.98	0.0334	0.998	54.35	2.1119	0.995
		75	82.81	83.37	0.0184	0.999	126.58	1.6750	0.988
	M2	25	28.96	28.85	0.0221	0.999	36.63	0.8669	0.995
		50	47.05	48.38	0.0292	0.998	54.35	2.1119	0.995
		75	43.90	44.52	0.0286	0.999	66.67	1.2279	0.991
	M3	25	26.63	28.14	0.0170	0.992	80.00	0.3259	0.962
		50	43.66	47.11	0.0269	0.992	71.43	0.9747	0.969
		75	38.47	39.25	0.0511	0.999	42.55	3.7092	0.998
MG	M1	25	23.10	24.13	0.0205	0.996	36.10	0.4684	0.990
		50	47.02	49.07	0.0154	0.981	79.37	0.7039	0.959
		75	64.13	69.25	0.0246	0.991	86.21	16.4069	0.984
	M2	25	19.80	20.22	0.0228	0.999	30.03	0.4523	0.991
		50	36.17	41.94	0.0249	0.984	55.56	0.7068	0.963
		75	56.80	54.31	0.0106	0.985	94.34	0.7780	0.903
	M3	25	9.98	10.79	0.0205	0.987	25.91	0.1367	0.970
		50	20.92	23.26	0.0214	0.982	43.29	0.3201	0.972
		75	39.28	41.64	0.0177	0.980	65.36	0.6468	0.978

Table 1 summarises the suitable results obtained from the two models. It can be seen from the results that the correlation coefficients of the pseudo-first-order model are higher than the pseudo-second-order. Thus, the pseudo-first-order-model was adopted to describe the process. Besides, the experimental adsorption capacities of two dyes onto mushrooms were closer to pseudo-first-order values. This result indicates that the number of free sites was significantly higher than the number of adsorbed dye molecules and reveals that the adsorption between dyes and biosorbents was physisorption which leads to a slow adsorption process. Furthermore, the pseudo-first-order model shows the effect of adsorption at the solid-liquid interface, indicating that the mushrooms had a certain affinity to the dye molecules (31).

Evaluation of biosorption isotherms

Two isotherm models namely, Freundlich and Langmuir, were used to identify the adsorption equilibrium. The equation for the Freundlich and Langmuir models predicated as in the Eqs.3 and 4:

$$\ln q_e = \ln K_F + (1/n_F)\ln C_e \quad (3)$$

$$C_e/q_e = 1/bq_m + C_e/q_m \quad (4)$$

where C_e is the equilibrium concentration (mg L^{-1}), q_e is the adsorption amount (mg g^{-1}) at equilibrium, q_m is the theoretical maximum adsorption capacity (mg g^{-1}) and *b* is Langmuir constant representing the enthalpy of sorption while K_F and n_F are the Freundlich constants related to the biosorption capacity (mg g^{-1}) and biosorption intensity or heterogeneity of the adsorbent, respectively. According to the Langmuir isotherm model, all the adsorption sites were the same and dynamically equivalent due to the monolayer adsorption. In the case of the Freundlich isotherm model, the adsorption caused by a heterogeneous mechanism. The calculated parameters of both models are summarized in Table 2 and it can be seen that the Freundlich isotherm model is well fitted with the biosorption of all mushrooms onto two dye processes because of their high R^2 values. Furthermore, the 1/n values which were in a range of 0-1 indicated favourability of the adsorption of the mushrooms onto the MB and MG dyes. The equilibrium isotherms are presented in Figure 7.

Table 2. Parameters for the Langmuir and Freundlich isotherm models

			Freundlich			Langmuir		
Dye	Mushroom	T (K)	K_F	n	R^2	q_m	*b*	R^2
MB	M1	303	9.34	1.76	0.9888	114.94	0.04	0.9818
		313	7.23	1.86	0.9868	87.72	0.04	0.9454
		323	5.87	1.86	0.9932	69.93	0.04	0.9931
	M2	303	5.71	1.62	0.9919	102.04	0.03	0.9715
		313	9.35	1.27	0.9972	142.86	0.01	0.9788
		323	2.59	1.43	0.9952	86.96	0.02	0.9715
	M3	303	2.75	1.29	0.9929	144.93	0.01	0.9089
		313	1.68	1.21	0.9928	80.65	0.01	0.9721
		323	1.34	1.20	0.9906	53.48	0.02	0.9727
MG	M1	303	2.51	1.25	0.9983	163.93	0.01	0.9614
		313	3.51	1.51	0.9977	69.93	0.06	0.9722
		323	2.48	1.44	0.9942	28.41	0.06	0.9744
	M2	303	2.03	1.21	0.9810	166.67	0.01	0.9799
		313	2.36	1.37	0.9870	100.00	0.01	0.9836
		323	1.86	1.43	0.9929	65.79	0.02	0.9927
	M3	303	1.87	1.23	0.9977	144.93	0.01	0.9727
		313	1.79	1.36	0.9906	77.52	0.01	0.9823
		323	1.50	1.40	0.9974	61.73	0.01	0.9781

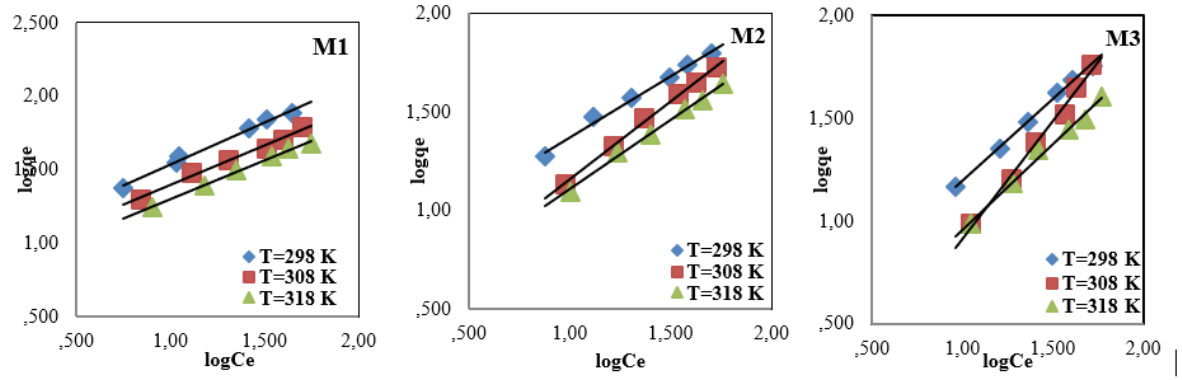

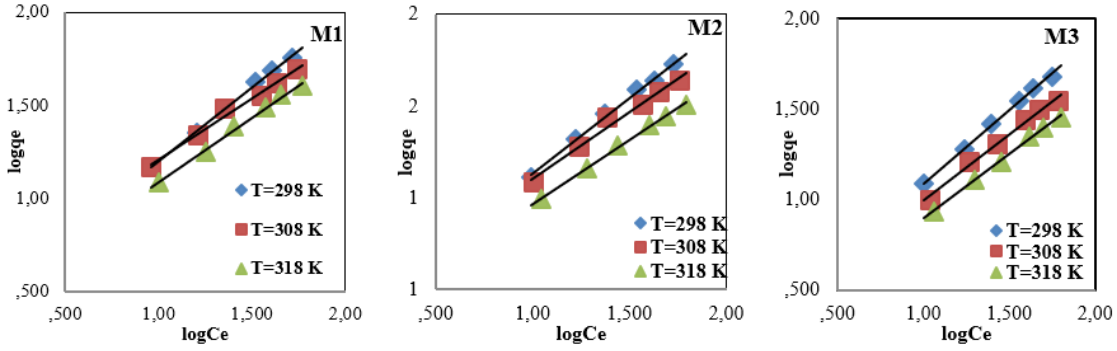

Figure 7. The plot of the Freundlich isotherm model **a:** MB, **b:** MG.

Besides, as shown in Table 2, theoretical adsorption capacity, q_m, decreased with increasing temperature remarking that the adsorptions of M1, M2, M3 on the MB and MG are favorable at lower temperatures. Also, the maximum adsorption capacities (Table 2) of M1, M2, M3 were determined as 82.81, 47.40 and 43.90 mg g^{-1} for MB and 64.13, 56.80 and 39.28 mg g^{-1} for MG adsorption at 303 K, respectively. Similarly, in the study of Yan and Wang (2013), the q_m was found as 63.5 mg g^{-1} for the adsorption of methylene blue by the spent mushroom substrate (32).

Thermodynamics of biosorption

To investigate the nature of the biosorption process of both cationic dyes onto M1, M2, M3, thermodynamic studies were applied. In this study, the thermodynamic equilibrium constant K_0 for the biosorption process was carried out by plotting $\ln(Q_e/C_e)$ versus Q_e in the temperature range of 303–323 K. Besides, thermodynamic parameters such as ΔH^0 enthalpy change and ΔS^0 entropy change were calculated from Eq.5 that was based on the slope and intercept of the Van't Hoff plots ($\ln K_0$ vs $1/T$, not shown) and the values of ΔG^0 Gibbs free energy change was calculated using Eq.6 (33):

$$\ln K = \Delta S^0/R - \Delta H^0/R\ (1/T) \quad (5)$$

$$\Delta G^0 = -RT\ln K_0 \quad (6)$$

where K_0 is the equilibrium constant, T is the solution temperature (K) and R is the gas constant (8.314 J mol^{-1} K^{-1}).

The related parameters are presented in Table 3. As can be seen from the table, the negative values of ΔG^0 show that the adsorption of two cationic dyes onto the mushrooms is spontaneous and feasible. The negative value of change in enthalpy (ΔH^0) indicates that the adsorption was an exothermic process. Since all values of ΔH^0 are smaller than 40 kJ/mol, the adsorption of MB and MG onto M1, M2 and M3 was a physisorption process. Furthermore, the positive value of change in entropy (ΔS^0) indicates the increasing randomness while negative value (MG adsorption of M2, M3) proves that the randomness of the solid/solution interface decreased during the adsorption process

Table 3. Thermodynamic parameters for MB, MG dyes on M1, M2, M3.

Dye	Mushroom	T (K)	ΔG(kJ/mol)	ΔH(kJ/mol)	ΔS(kJ/molK)
MB	M1	303	-24.82	-23.16	3.49
		313	-22.97		
		323	-24.97		
	M2	303	-24.75	-8.88	54.32
		313	-27.13		
		323	-25.76		
	M3	303	-26.57	-16.04	36.2
		313	-28.31		
		323	-27.24		
MG	M1	303	-24.57	-0.5	79.47
		313	-25.38		
		323	-26.16		
	M2	303	-26.85	-39.21	-60.01
		313	-25.67		
		323	-25.68		
	M3	303	-26.48	-38.12	-47.15
		313	-25.40		
		323	-25.53		

Table 4. Comparison of adsorption capacity of MB, MG dyes on M1, M2, M3 with other biosorbents.

Adsorbent	dye	Adsorption capacity (mg g^{-1})	Reference
Activated carbon	MG	57.03	(34)
Luffa aegyptica peel	MG	70.22	(35)
Pleurotus ostreatus	MG	32.35	(36)
Trichoderma viride	MB	201.50	(37)
Carica papaya wood	MG MB	52.63 32.25	(38)
Phellinus igniarius fungi	MB	232.21	(39)
Aspergillus fumigatus	MB	125.07	(40)
Corynebacterium glutamicum	MB	207.30	(41)
M1 M2 M3	MB	82.81 43.90 38.47	This study
M1 M2 M3	MG	64.13 56.80 39.28	This study

CONCLUSIONS

In the present study, the M1, M2 and M3 mushrooms were used as adsorbents for the investigation of MB and MG adsorption. The maximum adsorption capacity of M1, M2, M3 was found as 82.81, 43.90 and 38.47 mg g^{-1} for the MB dye and 64.13, 56.80 and 39.28 mg g^{-1} for the MG dye, respectively. The adsorption capacity of both dyes was found to increase with increasing pH from 3 to 11. The kinetic data were well fitted to pseudo-first-order. The isotherm data were in good agreement with the Freundlich isotherm model. All the results showed that the adsorption was exothermic. The studies in the literature also support the results of the present study by stating that the adsorption of MB and MG cationic dyes onto mushrooms is quite convenient.

REFERENCES

1. Wu J, Zhang T, Chen C, Feng L, Su X, Zhou L, Chen Y, Xia A, Wang X. Spent substrate of Ganodorma lucidum as a new bio-adsorbent for adsorption of three typical dye. Bioresource Technology. 2018; 266: 134–8.

2. Gao Y, Deng SQ, Jin X, Cai SL, Zheng SR, Zhang WG. The construction of amorphous metal-organic

cage-based solid for rapid dye adsorption and time-dependent dye separation from water. Chemical Engineering Journal. 2019; 357: 129–39.

3. Molla A, Li Y, Mandal B, Gu Kang S, Hur SH, Chung JS. Selective adsorption of organic dyes on graphene oxide: Theoretical and experimental analysis. Applied Surface Science. 2019; 464: 170–7.

4. Wang X, Jiang C, Hou B, Wang Y, Hao C, Wu JX. Carbon composite lignin-based adsorbents for the adsorption of dyes. Chemosphere 20. 2018; 6: 587-96.

5. Yeşilada Ö. Decolorization of Crystal Violet by Fungi, World Journal of Microbiology and Biotechnology. 1995; 11: 601-2.

6. Kunamneni A, Ghazi I, Camarero S, Ballesteros A, Plou FJ, Alcalde M. Decolorization of synthetic dyes by laccase immobilized on epoxyactivatedcarriers. Process Biochemistry. 2008; 43(2): 169-78.

7. Wesenberg D, Buchon F, Agathos SN. Degradation of Dye Containing Textile Effluent by Agaric White - Rot Fungus Clitocybula dusenii. Biotechnology Letters. 2002; 24: 989-93.

8. Stainer RY, Adelberg EA, Ingraham J. The Microbial World" Prentic Hall. Inc. Englewood Cliffs. New Jersey. 1976; 105-18.

9. Jaspers CJ, Penninck MJ. Adsorption Effects On the Decolorization of a Craftblach Plant Effluent by Phanerochaete chrysosporium. Biotechnology Letters. 1996; 11(18): 1257-60.

10. Couto SR. Rivela I. Munos MR, Sanroman A. Ligninolytic Enzyme Production and The Ability of Decolourisation of Poly R-478 in Packed Bed Bioreactors by Phanerochaete chrysosporium. Bioprocess Engineering.2000; 23: 287-93.

11. Wang Y, Yu J. Adsorption and Degradation of Synthetic Dyes on the Mycelium of Trametes versicolor. Water Science Technology. 1998; 4-5(38): 233-8.

12. Poverenov E, Arnon-Rips H, Zaitsev Y, Bar V, Danay O, Horev B, Bilbao-Sainz C, McHugh T, Rodo V. Potential of chitosan from mushroom waste to enhance quality andstorability of fresh-cut melons. Food Chemistry. 2018; 268: 233–41.

13. Kurt A, Gençcelep H. Enrichment of meat emulsion with mushroom (Agaricus bisporus) powder: Impact on rheological and structural characteristics. Journal of Food Engineering. 2018; 237: 128–36.

14. Sewu DD, Boakye P, Jung H, Woo SH. Synergistic dye adsorption by biochar from co-pyrolysis of spent mushroom substrate and Saccharina japonica. Bioresource Technology. 2017; 244: 1142–9.

15. Kariuki Z, Kiptoo J, Onyanch D. Biosorption studies of lead and copper using rogers mushroom biomass 'Lepiota hystrix'. South african journal of chemical engineering. 2017; 23: 62-70.

16. Kamasonlian S, Balomajumder C, Chand S, Suresh S. Biosorption of Cd(II) and As(III) ions from aqueous solution by tea waste biomass. Afr. J. Environ. Sci. Technol. 2011; 5(1):1-7.

17. Negm NA, Wahed MGAE, Hassan ARA, Kana MTHA. Feasibility of metal adsorption using brown algae and fungi: Effect of biosorbents structure on adsorption isotherm and kinetics Journal of Molecular Liquids. 2018; 264: 292–305.

18. Auta M, Hameed BH. Chitosan-clay composite as highly effective and low cost adsorbent for bathch and fixed-bed adsorption of methylene blue. Chemical Engineering Journal. 2014; 237: 352-61.

19. Karadirek Ş, Okkay H. Statistical modeling of activated carbon production from spent mushroom compost. Journal of Industrial and Engineering Chemistry. 2018; 63: 340–7.

20. Hu S, Hsieh Y. Preparation of Activated Carbon and Silica Particles from Rice Straw. ACS Sustain, Chem. Eng. 2014; 2(4): 726.

21. Mahmoud ME, Nabil GM,. El-Mallah NM, Bassiouny HI, Kumar S, Abdel-Fattah TM. Kinetics, isotherm, and thermodynamic studies of the adsorption of reactive red 195 A dye from water by modified Switchgrass Biochar adsorbent. J. Ind. Eng. Chem. 2016; (37) 156. https://doi.org:10.1016/j.jiec.2016.03.020.

22. Budnyak TM, Aminzadeh S, Pylypchuk IV, Sternik D, Tertykh VA, Lindström ME, Sevastyanova O. Methylene Blue dye sorption by hybrid materials from technical lignins. Journal of Environmental Chemical Engineering. 21018; 6: 4997–5007.

23. Zahira A, Aslam Z, Kamal MS, Ahmad W, Abbas A, Shawabk RA. Development of novel cross-linked chitosan for the removal of anionic Congo red dye. Journal of Molecular Liquids. 2017; 244: 211–8.

24. Singh S, Gaikwad KK, Lee M, Lee YS. Thermally buffered corrugated packaging for preserving the postharvest freshness of mushrooms (Agaricus bispours). Journal of Food Engineering. 2018; 216: 11-9.

25. Tong DS, Wu CW, Adebajo MO, Jin GC, Yu WH, Ji SF, Zhou CH. Adsorption of methylene blue from aqueous solution onto porous cellulose derived carbon/montmorillonite nanocomposites. Applied Clay Science. 2018; 161(1): 256-64.

26. Auta M, Hameed BH. Chitosan–clay composite as highly effective and low-cost adsorbent for batch and fixed-bed adsorption of methylene blue. Chemical Engineering Journal. 2014; 237: 352–61.

27. Liu X, Lee DJ. Thermodynamic parameters for adsorption equilibrium of heavy metals and dyes from wastewaters. Bioresource Technology. 2014; 160: 24–31.

28. Ishmaturrahmi R, Mustafa I. Methylene blue removal from water using H2SO4 crosslinked magnetic chitosan nanocomposite beads. Microchemical Journal. 2019; 144: 397–402.

29. Ho YS, McKay G. Review of second-order models for adsorption systems, Chem. Eng. J. 1998; 70: 115–24. https://doi.org/10.1016/j.jhazmat.2005.12.043.

30. Ho YS, McKay G. Pseudo-second order model for sorption processes, Process Biochem. 1999; 34: 451–65, https://doi.org/10.1016/S0032-9592(98)00112-5.

31. Ai T, Jianga X, Liu Q, Lv L, Wu H. Daptomycin adsorption on magnetic ultra-fine wood-based biochars from water: Kinetics, isotherms, and mechanism studies. Bioresource Technology. 2019; 273: 8–15.

32. Yan T, Wang L. Adsorptive Removel of Methylene blue from Aqueous Solution by spent mushroom substrate: Equilibrum, Kinetics, and Thermodynamics. BioResources. 2013; 8(3): 4722-34.

33. Wong S, Tumari HH, Ngadi N, Mohamed NB, Hassan O, Mat R, Amin NAS. Adsorption of anionic dyes on spent tea leaves modified withpolyethyleneimine (PEI-STL). Journal of Cleaner Production. 2019; 206: 394-406.

34. Rahman IA, Saad B, Shaidan, Sya Rizal E S . Adsorption characteristics of malachite green on activated carbon derived from rice husks produced by chemical–thermal process. Bioresource Technology. 2005; 96(14):1578-83.

35. Mashkoor F, Nasar A. Preparation, characterization and adsorption studies of the chemicallymodifiedLuffa aegypticapeel as a potential adsorbent for the removal ofmalachite green from aqueous solution. Journal of Molecular Liquids. 2019; 274:315–27.

36. Chen Z, Deng H, Chen C, Yang Y, Xu H. Biosorption of malachite green from aqueous solutions by Pleurotus ostreatus using Taguchi method. Journal of Environmental Health Science & Engineering. 2014; 12: 63.

37. Saeed A, Iqbal M, Zafar S I. Immobilization of Trichoderma viride for enhanced methylene blue biosorption: Batch and column studies. Journal of Hazardous Materials. 2009; 168(1): 406-15.

38. Rangabhashiyam S, Lata S, Balasubramanian P. Biosorption characteristics of methylene blue and malachite green from simulated wastewater onto Carica papaya wood biosorbent. Surfaces and Interfaces. 2018; 10: 197-215.

39. Maurya N S, Mittal A K, Cornel P, Rother E. Biosorption of dyes using dead macro fungi: Effect of dye structure, ionic strength and pH. Bioresource Technolog. 2006; (7)3:512-21.

40. Abdallah R, Taha S. Biosorption of methylene blue from aqueous solution by nonviable Aspergillus fumigatus. Chemical Engineering Journal. 2012; 195–196, 69-76.

41. Vijayaraghavan K, Won S W, Mao J, Yun Y-S. Chemical modification of Corynebacterium glutamicum to improve methylene blue biosorption. Chemical Engineering Journal.2008; 145(1): 1-6.